

# **Shielding Assessment for Electron Gun Commissioning at the New Muon Lab**

Mike Church

**April 3, 2012**

# Table of Contents

<b>1</b>	<b>INTRODUCTION.....</b>	<b>3</b>
1.1	DESCRIPTION OF FACILITY .....	3
1.2	BEAM CONDITIONS.....	5
1.2.1	<i>Simulations for laser-induced beam</i> .....	6
1.2.2	<i>Simulations for dark current</i> .....	6
<b>2</b>	<b>PROMPT RADIATION.....</b>	<b>8</b>
2.1	NORMAL OPERATIONS.....	8
2.1.1	<i>Radiation source terms</i> .....	8
2.1.2	<i>Dose rates outside shielding</i> .....	9
2.1.3	<i>Labyrinth calculation</i> .....	10
2.1.4	<i>Penetrations</i> .....	11
2.1.5	<i>Conclusions</i> .....	11
<b>3</b>	<b>REFERENCES.....</b>	<b>13</b>
<b>4</b>	<b>APPENDICES.....</b>	<b>14</b>
4.1	SHIELDING DRAWINGS .....	14

# 1 Introduction

## 1.1 Description of facility

The electron gun is located at the upstream (south) end of the NML beamline enclosure as shown in Figure 1.1. The gun itself is a cylindrical copper 1½ cell L-band (1.3 GHz) cavity identical to the type IV gun developed by DESY/PITZ and currently in use at FLASH [1]. Electrons are emitted from a photocathode excited by a UV laser pulse of wavelength 254nm and accelerated in the gun by the RF field. The laser pulse is directed onto the photocathode via a mirror located 0.98m downstream of the photocathode.

The gun is mounted on a stand which also supports 2 solenoid magnets used for beam focusing. These solenoids will be operated at a variety of currents during commissioning.

The upstream end of the gun is attached to a cathode transfer chamber used to insert cathodes into the gun. A variety of Mo cathodes, some uncoated and some coated with Cs<sub>2</sub>Te, will be used during the commissioning.

The gun is cooled by an LCW water skid located in the tunnel at the upstream end of the NML service floor. The gun is designed to dissipate up to 30KW of DC power and will operate under tight temperature feedback control in order to maintain RF phase stability.

During initial commissioning a Faraday cup will be attached directly to the downstream end of the gun and will be located 0.80m downstream of the photocathode plane. This Faraday cup consists of a 13.5mm thick stainless steel flange followed by a 31.5mm thick copper disk, similar to what is currently installed on both ends of CC-2 at NML. At a later date, this Faraday cup will be replaced with an insertable Faraday cup 1.35m downstream of the photocathode plane. This 2<sup>nd</sup> Faraday cup consists of a copper cylinder ~30mm in diameter. Both Faraday cups will be instrumented to measure beam current, and will be monitored during commissioning.

RF power is supplied by a 5MW 1.3GHz power supply/modulator/transformer/klystron located on the NML service floor just outside the beam enclosure's upstream access gate. This system is very similar to the RF system currently driving CM-1 at NML. The power distribution system consists of waveguide, a circulator, and an RF waveguide switch. Power is coupled to the gun cavity via an RF vacuum window and coaxial coupler located on the downstream end of the gun.

Figure 1.2 shows a cross sectional view of the gun and vicinity. The 2<sup>nd</sup> Faraday cup, laser mirror, and other instrumentation is contained in the "9-way cross" assembly shown in this drawing. The 9-way cross assembly will not be installed until initial conditioning of the gun cavity is complete, hence, the initial commissioning will be done with "dark current" only – current emitted from the inner surfaces of the cavity due to high electric fields.

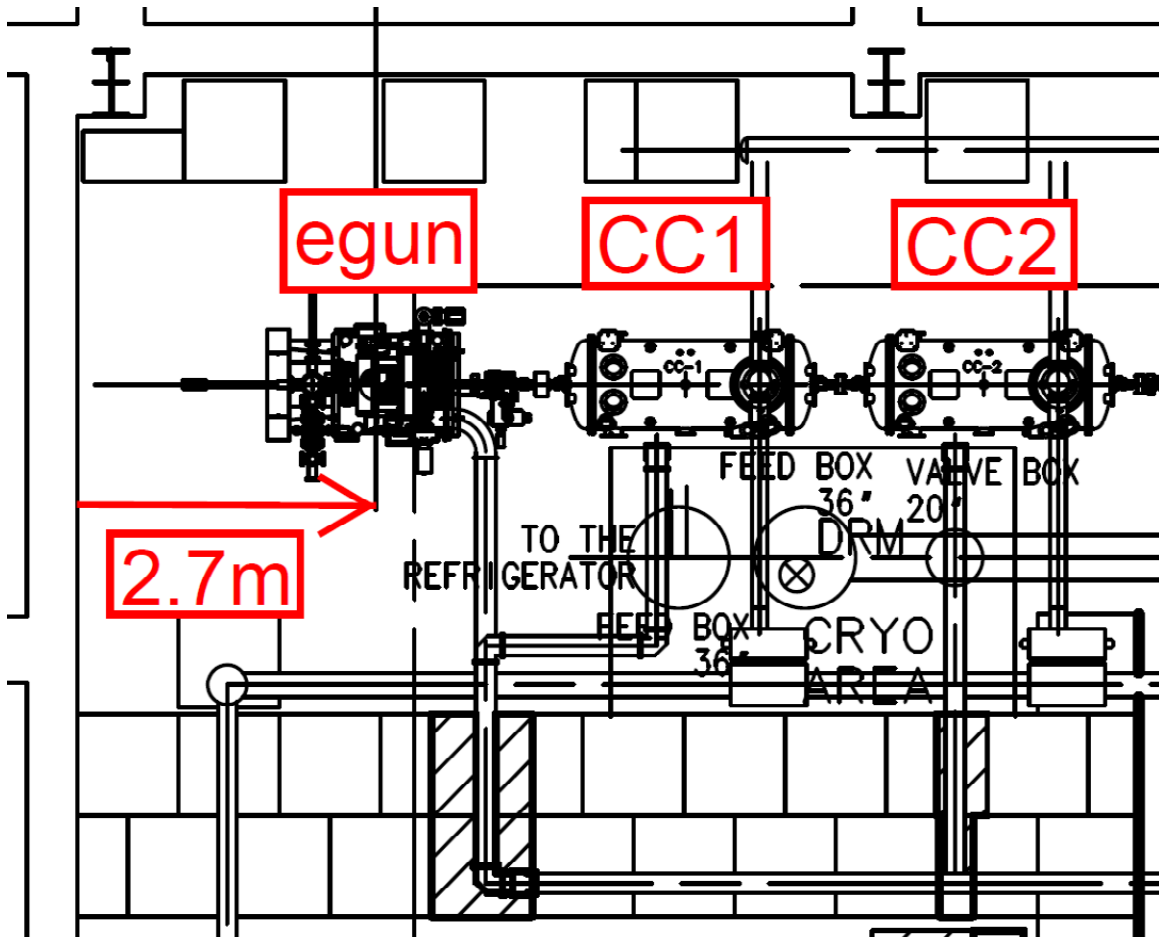


Figure 1.1: Plan view of location of electron gun at the upstream end of the NML beamline enclosure. CC2 is currently installed, but CC1 will not be installed until after gun commissioning. The photocathode plane is 2.7m from the NML south wall and is 1.22m above the floor. Appendix 4.1 shows a more general NML floor plan.

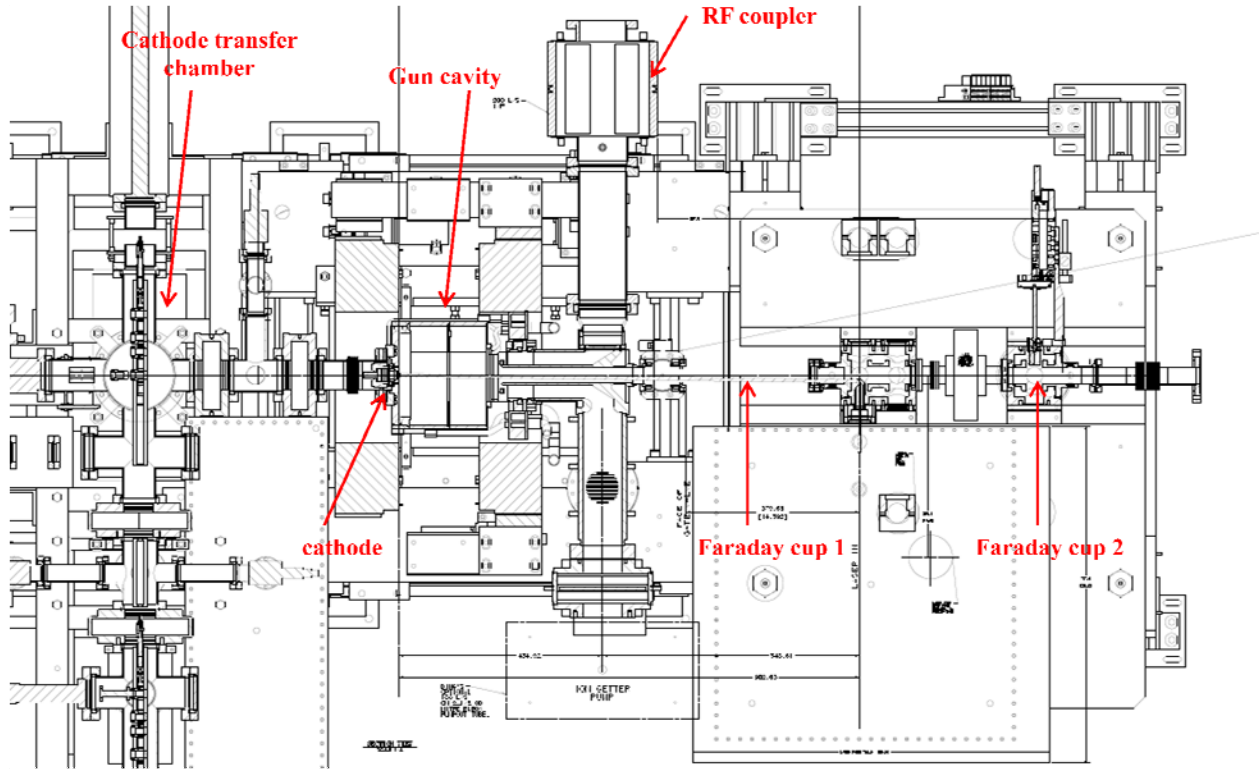


Figure 1.2: Cross-sectional plan view of the electron gun, coupler, and downstream instrumentation.

## 1.2 Beam conditions

Gun commissioning will consist of driving the gun with RF at gradually increasing power levels, varying repetition rates (maximum of 5Hz), and varying pulse widths (maximum of 1msec). We start with low power, short pulse length, and low repetition rate and gradually increase the power as the gun “conditions” -- i.e., sparking and vacuum bursts are reduced to acceptable levels. Initial stages of commissioning will be done with “dark current” only – i.e., a laser pulse will not be incident on the photocathode until later stages of commissioning. Dark current consists of electrons emitted by the internal surfaces of the cavity in the presence of high field gradients.

Dark current intensity exiting the gun varies dramatically from cathode to cathode. Measurements at DESY/PITZ over the past few years show variations from  $\sim 20\mu\text{A}$  to  $1\text{mA}$  [2,3,4] at these field gradients. Our own recent experience at A0PI shows variations from  $5\mu\text{A}$  to  $500\mu\text{A}$  at somewhat lower field gradients. Based on the recent DESY/PITZ experience, we will assume a maximum of  $1\text{mA}$  of dark current exiting the gun for this shielding assessment. We will limit the laser-induced photocurrent to  $1\text{mA}$  due to the limited heat dissipation capability of the Faraday cups. Therefore the total maximum beam current (dark current + photocurrent) exiting the gun is  $2\text{mA}$ . The maximum duty cycle =  $1\text{msec}$  pulse at  $5\text{Hz}$  =  $0.005$ , therefore **the maximum average current exiting the gun is  $10\mu\text{A}$** . This corresponds to  $54\text{W}$  of

beam power at the maximum gun gradient, which will probably challenge the radiant and conductive cooling capacity of the Faraday cups.

The gun is driven by a 5MW klystron. However, due to losses in the waveguide, circulator, RF switch, and RF window, a maximum of 4.6MW can be delivered to the gun cavity itself [5]. This corresponds to a peak electric field at the photocathode of 50.6MV/m [6].

ASTRA (A Space Charge Tracking Algorithm) [7] simulations are done separately for laser-induced beam and dark current to determine the range of beam conditions.

### 1.2.1 Simulations for laser-induced beam

At the maximum peak electric field and for an incident laser pulse timed for maximum acceleration, the outgoing beam has a kinetic energy of 5.4 MeV. The kinetic energy spectrum is shown in Figure 1.3. **We therefore use a monoenergetic beam of 5.4MeV kinetic energy for laser-induced forward emitted beam for this shielding assessment.**

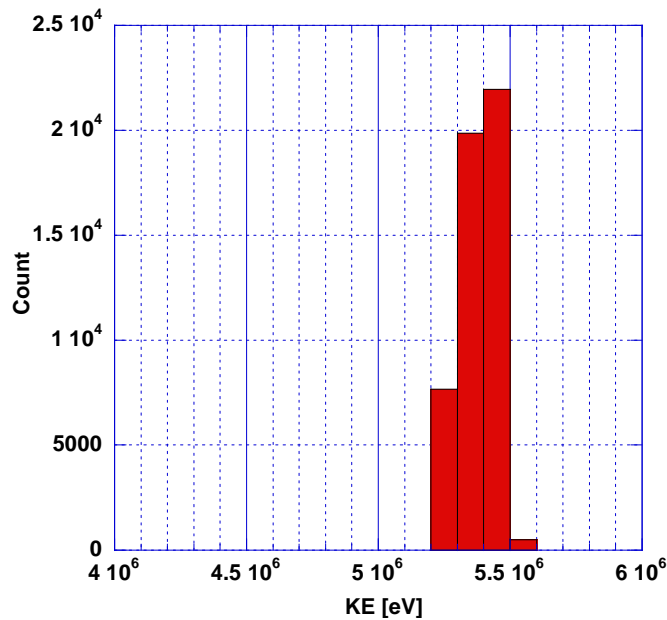


Figure 1.3: Kinetic energy distribution of laser-induced beam out of the gun at the peak gradient of 50.6MV/m from ASTRA simulation.

### 1.2.2 Simulations for dark current

We use the Fowler-Nordheim model [8] for electron emission from surfaces in high electric fields. Dark current from an RF gun has been extensively investigated in [9] and we use a similar model as that reference for field emission near the photocathode. Only dark current originating near the photocathode can exit the gun.

At peak field gradients and at most solenoid strengths, ~100% of the dark current reaches the Faraday cup. The kinetic energy spectrum of the dark current is shown in Figure 1.4. The dark current has a lower energy spectrum than the laser-induced beam, however **we will use a**

monoenergetic beam of 5.4MeV kinetic energy for forward emitted dark current for this shielding assessment.

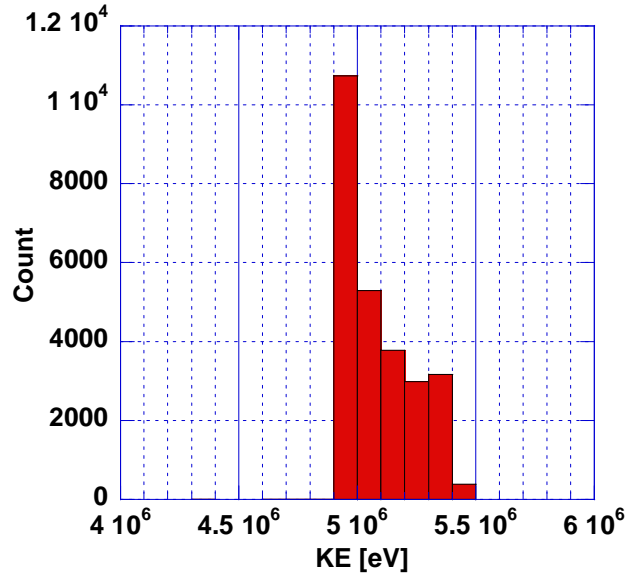


Figure 1.4: : Kinetic energy distribution of dark current out of the gun at the peak gradient of 50.6MV/m from ASTRA simulation.

In addition to dark current originating from the photocathode region, dark current can also originate from the high field regions of the gun upstream iris and exit iris. However, this beam cannot exit the gun, and is driven into the walls of the cavity by the RF fields [9]. We estimate that this current (in a given radial direction) is a maximum of 100% of the exiting dark current and with a peak kinetic energy of 2MeV [10]. **Therefore the maximum average dark current within the gun, at right angles to the exiting beam axis, is  $5\mu\text{A}$ , with a kinetic energy of 2MeV.**

## 2 Prompt radiation

### 2.1 Normal operations

#### 2.1.1 Radiation source terms

For this shielding assessment we use the methodology outlined in NCRP Report #51 [11]. In this chapter we refer to appendices and page numbers in that report. The beam energy is well below the neutron production threshold for common materials [12], therefore radioactivation (water, air, or materials) and the tracking of neutrons are not of concern in this shielding assessment.

From NCRP#51 Appendix E.1 (pg. 95) the X-ray emission rates from a high-Z target are:

$9.6 \times 10^3$  rad-m<sup>2</sup>/mA/min: 5.4MeV, 0° from exiting beam axis (0° from incident electrons);

$1.7 \times 10^2$  rad-m<sup>2</sup>/mA/min: 2.0MeV, 0° from exiting beam axis (90° from incident electrons);

$7.5 \times 10^2$  rad-m<sup>2</sup>/mA/min: 5.4MeV, 90° from exiting beam axis (90° from incident electrons);

$3.9 \times 10^2$  rad-m<sup>2</sup>/mA/min: 2.0MeV, 90° from exiting beam axis (0° from incident electrons).

From NCRP#51 Appendix E.3 (pg. 98) scale the 1<sup>st</sup> and 4<sup>th</sup> terms by 0.7 and scale the 2<sup>nd</sup> and 3<sup>rd</sup> terms by 0.5 for iron or copper targets. Multiply the 1<sup>st</sup> and 3<sup>rd</sup> terms by 10 μA, multiply the 2<sup>nd</sup> and 4<sup>th</sup> terms by 5 μA, and convert to hours and mrad to obtain 4 source terms (particle fluence rates) for 0° and 90°:

$4.03 \times 10^6$  mrad-m<sup>2</sup>/hr: 5.4MeV, 0° from exiting beam axis (0° from incident electrons);

$2.55 \times 10^4$  mrad-m<sup>2</sup>/hr: 2.0MeV, 0° from exiting beam axis (90° from incident electrons);

$2.25 \times 10^5$  mrad-m<sup>2</sup>/hr: 5.4MeV, 90° from exiting beam axis (90° from incident electrons);

$8.19 \times 10^4$  mrad-m<sup>2</sup>/hr: 2.0MeV, 90° from exiting beam axis (0° from incident electrons).

In order to estimate the 5.4MeV source terms for angles between 0° and 90°, we first fit the 8MeV and 3MeV plots of source term vs. angle in NCRP#51 Appendix E.2 (pg. 97) with the parameterization

$$\text{source term} = 100000 / (c1 + c2 * \theta + c3 * \theta^2 + c4 * \theta^3).$$

The constants in these fits are then logarithmically interpolated to obtain constants for a 5.4MeV curve, and adjusted slightly to make the 0° and 90° values match those given above. Figure 2.1 shows these fits. The 5.4MeV curve is then multiplied by beam current and the appropriate copper/iron target factor – a factor of 0.7 is used for angles less than 60°, and a factor of 0.7 to 0.5 is used for angles between 60° and 90°, scaled linearly between those two values. The final formula for the 5.4MeV source term is then (with  $\theta$  in degrees)

$$6.0 * 10^7 * (0.7) / (10.417 + 0.467 * \theta + 0.0188 * \theta^2 - 9.81 * 10^{-5} * \theta^3) \text{ [mrad-m}^2\text{/hr] for } \theta < 60,$$

$$6.0 * 10^7 * (1.1 - 0.00666 * \theta) / (10.417 + 0.467 * \theta + 0.0188 * \theta^2 - 9.81 * 10^{-5} * \theta^3) \text{ [mrad-m}^2\text{/hr] for } 60 < \theta < 90.$$

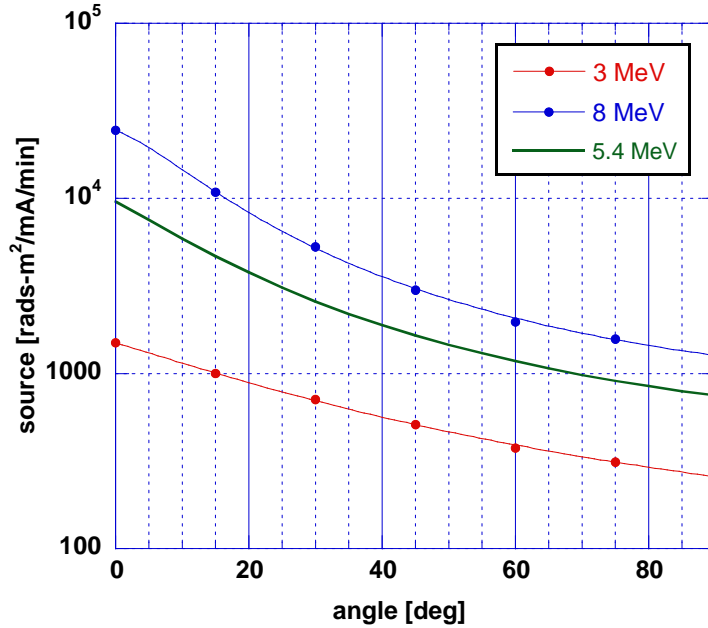


Figure 2.1: Fits to x-ray emission rates for 3MeV and 8MeV and interpolation to 5.4MeV. Data points are from NCRP#51 Appendix E.2.

### 2.1.2 Dose rates outside shielding

Per NCRP#51 Appendix E.6 (pg. 101), for radiation emitted at  $90^\circ$  from the incident electron, the equivalent energy to use for 5.4MeV is 3.4MeV for transmission calculations. We do not apply this correction to the 2.0MeV source terms.

The dose rate outside the shielding is [11]

$$D = (\text{source term}) * 0.1 * 10^{-(\Delta-\delta_1)/\delta} / r^2,$$

where  $\Delta$  is the thickness of the shielding [m],  $\delta_1$  is the 1<sup>st</sup> 1/10<sup>th</sup> value layer [m],  $\delta$  is the subsequent 1/10<sup>th</sup> value layer [m], and  $r$  is the distance from the source to the point where the dose rate is measured [m]. The enclosure shielding is concrete with density = 2.35g/cm<sup>2</sup> and 1/10<sup>th</sup> value layers have been taken from NCRP#51 Appendix E.12 (pg. 107). Table 2.1 shows the calculated dose rates at a number of locations outside the enclosure. Refer to the drawings in the appendices for shielding layout and cross sections. Pts. 1-5 are outside the enclosure walls; pts. 6-8 are above the enclosure roof; pt. 9 is outside the west wall of the NML building; and pt. 10 is on the laser hut roof. Pt. 9 has both concrete and soil shielding, and the density of soil is taken to be 1.8g/cm<sup>2</sup> and its 1/10<sup>th</sup> value layer is scaled accordingly from concrete and taken as 0.35m in this case.

Table 2.1: Dose limits outside the NML enclosure. Pts. 1-5 are above the service floor (beamline ht. = 1.22m); pts. 6-8 are on the enclosure roof, directly above the beamline; pt. 9 is outside the west wall of the NML building; and pt. 10 is on the laser hut roof. Pt. 9 has both concrete and soil as shielding. Refer to appendices for locations. We are assuming Q=1 in converting from mrad to mrem.

pt. #	plane	angle [deg]	equivalent Energy [MeV]	1st 1/10th value thickness [m]	1/10th value thickness [m]	distance [m]	shield thickness [m]	cross section used	source term [mrad-m <sup>2</sup> /hr]	dose [mrem/hr]	dose sum [mrem/hr]
1	H	0	5.4	0.335	0.335	45.1	1.83	plan view	4.03E+06	0.007	0.007
			2.0	0.225	0.205				2.55E+04	0.000	
2	H	16	5.4	0.335	0.335	24.3	6.64	plan view	1.88E+06	0.000	0.000
			2.0	0.225	0.205				2.55E+04	0.000	
3	H	36	5.4	0.335	0.335	11.4	3.11	plan view	8.93E+05	0.000	0.000
			2.0	0.225	0.205				2.55E+04	0.000	
4	H	58	5.4	0.335	0.335	5.7	2.16	plan view	5.15E+05	0.006	0.006
			2.0	0.225	0.205				8.19E+04	0.000	
5	H	90	3.4	0.270	0.270	4.7	1.83	2.4 m	2.25E+05	0.002	0.002
			2.0	0.225	0.205			x-sec.	8.19E+04	0.000	
6	V	20	5.4	0.335	0.335	7.9	2.67	14.1 m	1.59E+06	0.000	0.000
			2.0	0.225	0.205			x-sec.	2.55E+04	0.000	
7	V	66	5.4	0.335	0.335	4.2	1.00	6.7 m	4.17E+05	24.491	24.568
			2.0	0.225	0.205			x-sec.	8.19E+04	0.077	
8	V	90	3.4	0.270	0.270	2.9	0.91	2.4 m	2.25E+05	11.403	11.847
			2.0	0.225	0.205			x-sec.	8.19E+04	0.444	
9	44	90	3.4	0.270	0.270	7.2	1.35	2.4 m	2.25E+05	0.000	0.000
(outside NML)			soil-->	0.350	0.350		2.70	x-sec.			
10	45	90	3.4	0.270	0.270	6.0	1.27	2.4 m	2.25E+05	0.124	0.124
(laser deck)								x-sec.			

### 2.1.3 Labyrinth calculation

The upstream NML enclosure access labyrinth is well protected from direct x-rays from the Faraday cup source by a 3'x3'x7.5' concrete block just upstream of the labyrinth entrance. In addition, radiation will have to be reflected 3 times in order to exit the labyrinth, as shown in Figure 4.1. We use NCRP#51 eq. 7 (p. 53) to estimate the source term after the 1<sup>st</sup> reflection in the labyrinth:

$$S_r = S * \alpha * A / d^2 = 2.7 \times 10^2 \text{ mrem-m}^2/\text{hr.}$$

Here S is the target source term =  $1.16 \times 10^6$  mrem-m<sup>2</sup>/hr for 5.4MeV electrons at 28° (ignoring the attenuation by the 3'x3'x7.5' concrete block);  $\alpha$  is the reflection coefficient taken from NCRP#51 Appendix E15 (pg. 11) to be 0.007; A is the radiation-illuminated area (taken as  $3' \times 7.5' = 2.1\text{m}^2$ ), and d= 7.4m is the distance from the source to the labyrinth wall. Then applying NCRP#51 eq. 13 (pg. 63) to the 3 legs of the labyrinth (d = 1.4m, 2.7m, 1.8m) and now using  $\alpha = 0.02$  gives the dose rate at the labyrinth exit:

$$D_{\text{exit}} = 0.012 \text{ mrem/hr.}$$

### 2.1.4 Penetrations

There are two penetrations of concern, one on the east side of enclosure and one on the west side of the enclosure.

On the west side, there is a 3'x2' gap between the roof blocks and the west NML wall (see Fig. 4.5) almost directly across from the Faraday cup and between the west wall enclosure pillars shown in Fig. 4.1. X-rays from the target can strike the west wall and reflect up through this gap. Again we use NCRP#51 eq. 13 (pg. 63) to calculate the dose on the enclosure roof:

$$D = S * \alpha * A / d_1^2 / d_r^2 = 21.5 \text{ mrem/hr.}$$

S is the target source term =  $2.25 \times 10^5$  mrem-m<sup>2</sup>/hr for 5.4MeV source electrons at 90°;  $\alpha$  is the reflection coefficient taken from NCRP#51 Appendix E15 (pg. 11) to be 0.003; A is the radiation-illuminated area (taken as 3'x7.5' = 2.1m<sup>2</sup>),  $d_1$  = 2.8m is the distance from the source to the west wall, and  $d_r$  = 2.9m is the distance from the west wall up through the shielding gap to the enclosure roof. We ignore the attenuation in the steel plate at the top of the gap.

On the east side there is a 3'x3' penetration (shown in Fig. 1.1) filled with cinder blocks but containing a 1.3GHz waveguide, several small conduits for cables, and 5.5" O.D. vacuum pipe for the gun laser light transmission. We use the laser vacuum pipe in this dose estimate, since it has the largest cross section. The entrance to the penetration is 4.2m from the source, the angle from the source to the penetration is 44° from the horizontal, and the penetration length is 1.8m. We use the same prescription as the west side penetration to estimate the dose outside this penetration:

$$D = S * \alpha * A / d_1^2 / d_r^2 = 0.83 \text{ mrem/hr.}$$

S is the target source term =  $2.25 \times 10^5$  mrem-m<sup>2</sup>/hr for 5.4MeV source electrons at 90°;  $\alpha$  is the reflection coefficient taken from NCRP#51 Appendix E15 (pg. 11) to be 0.014 for this angle for steel; A is the radiation-illuminated area (taken as the area of the laser light pipe = 0.015m<sup>2</sup>),  $d_1$  = 4.2m is the distance from the source to the penetration entrance, and  $d_r$  = 1.8m is the distance through the penetration.

### 2.1.5 Conclusions

- 1) The gun internal dark current is a negligible contributor to overall dose rates. The dose rates are dominated by the Faraday cup source at 5.4MeV.
- 2) Dose rates on the NML service floor are below the 0.25mrem/hr limit required for "Signs (CAUTION – Controlled Area). No occupancy limits imposed." [FRCM, Table 2-6].
- 3) The dose rate outside the upstream east wall penetration can be classified as "Signs (CAUTION – Controlled Area) and minimal occupancy." [FRCM, Table 2-6]. This area can only be reached via a ladder.
- 4) By far the highest possible dose rates are on the enclosure roof, directly above the Faraday cup. These rates are within the classification "Signs (CAUTION – Radiation Area) and rigid barriers with locked gates." [FRCM, Table 2-6].
- 5) We recommend that a chipmunk be placed on the enclosure roof ~4m from the south building wall and interlocked to the gun RF power source.

- 6) There already exists a chipmunk on the east enclosure wall at the penetration opposite the gun, and we recommend that this be interlocked to the gun RF power source also.
- 7) We recommend that appropriate radiation warning signs be placed on the barriers atop the enclosure walls all around the enclosure.

### 3 References

- [1] F. Stephan *et al.*, “Detailed Characterization of Electron Sources Yielding First Demonstration of European X-ray Free-Electron Laser Beam Quality”, *Phys. Rev. ST Accel. Beams* **13**, 020704 (2010).
- [2] A. Oppelt *et al.*, “Tuning, Conditioning, and Dark Current Measurements of a New Gun Cavity at PITZ” (THPPH023) in *Proceedings of FEL 2006*, Berlin, Germany (2006)
- [3] L. Monaco *et al.*, “Dark Current Investigations of FLASH and PITZ RF Guns” (WEPLS051) in *Proceedings of EPAC 2006*, Edinburgh, Scotland (2006)
- [4] M. Otevrel, *et al.*, “Conditioning of a new Gun at PITZ Equipped with an Upgraded RF Measurement System” in *Proceedings of FEL2010 Malmo*, Sweden (2010)
- [5] J. Reid, private communication (3/12/2012)
- [6] S. Lederer *et al.*, “Conditioning of a New Gun Cavity Towards 60 MV/m at PITZ” (TUPMN026) in *Proceedings of PAC07*, Albuquerque, New Mexico (2007)
- [7] K. Floettman, “ASTRA – A Space Charge Tracking Algorithm”, [www.desy.de/~mpyflo](http://www.desy.de/~mpyflo)
- [8] R.H. Fowler, L. Nordheim, “Electron Emission in Intense Electric Fields” in *Proc. R. Soc. A*, 119, May 1928, London, pp 173-181
- [9] L. Frohlich, DESY-Thesis-2009-012/TESLA-FEL 2009-3, DESY, Hamburg, Germany, May 2009
- [10] M. Huening, “A0 North Cave Radiation Shield Calculations – Rev. 3”, 2/19/2004
- [11] NCRP Report #51, “Radiation Protection Guidelines for 0.1 – 100 MeV Particle Accelerator Facilities”
- [12] NCRP Report #79, “Neutron Contamination from Medical Electron Accelerators” (p 4)

## 4 Appendices

### 4.1 Shielding drawings

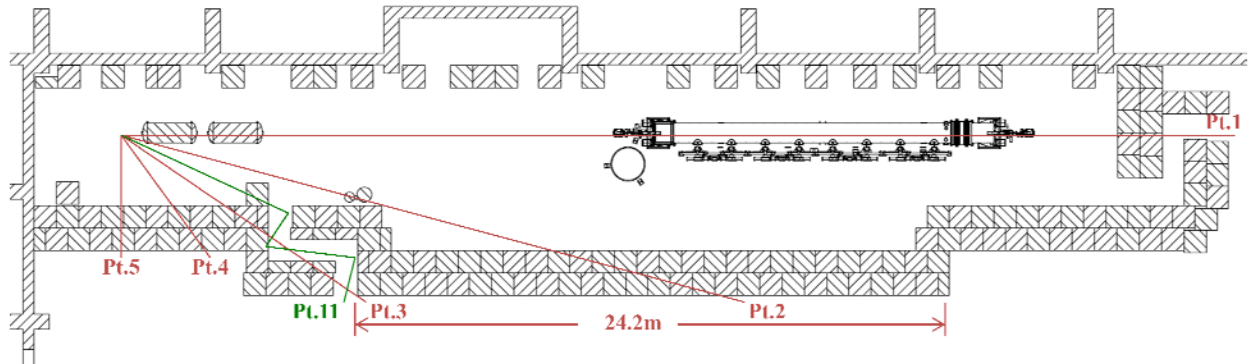


Figure 4.1: Plan view of enclosure at beam height (1.22m). Shown are the points where dose rates are tabulated in Table 2.1. Green trace and Pt. 11 refer to the labyrinth calculation.

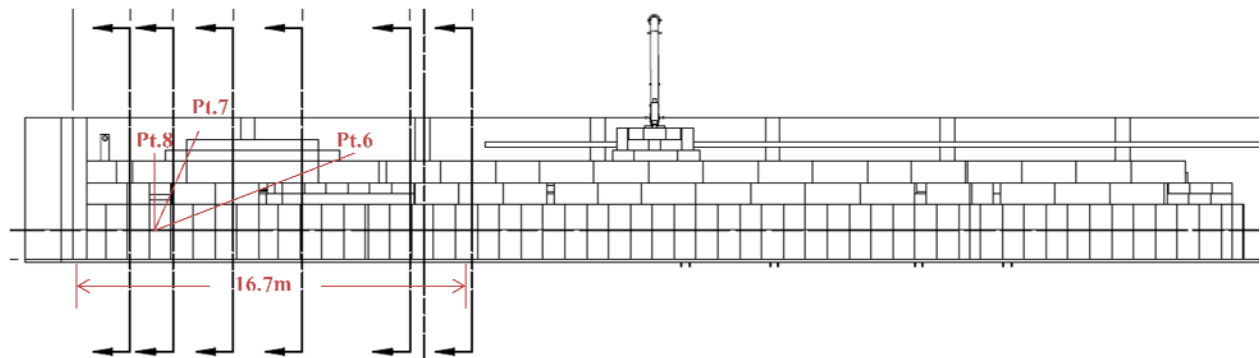


Figure 4.2: Elevation view of enclosure. Shown are the enclosure roof points where dose rates are tabulated in Table 2.1.

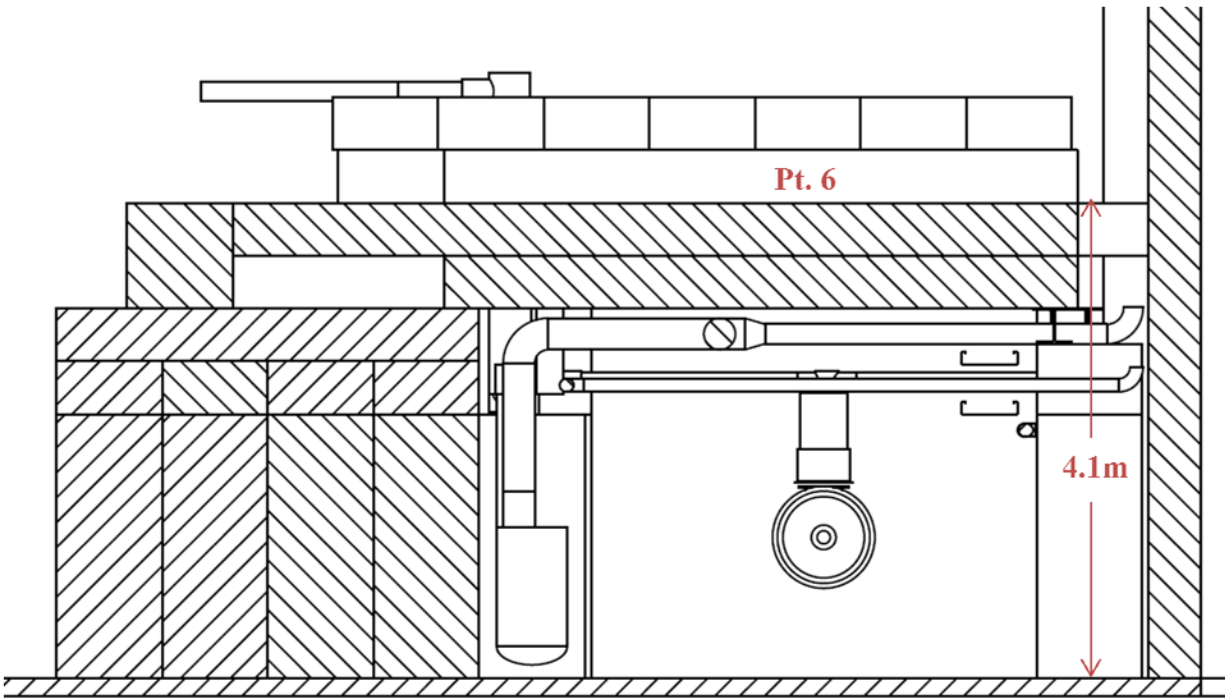


Figure 4.3: Cross section of tunnel enclosure at dose pt. 6.

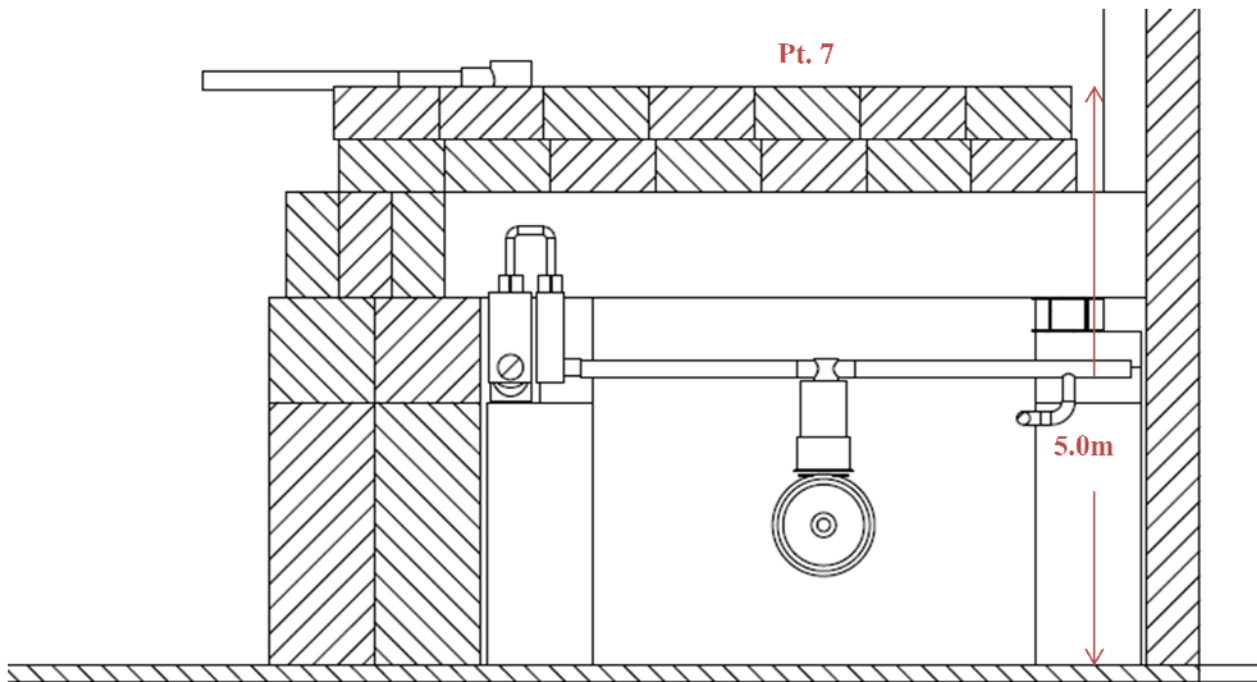


Figure 4.4: Cross section of tunnel enclosure at dose pt. 7.

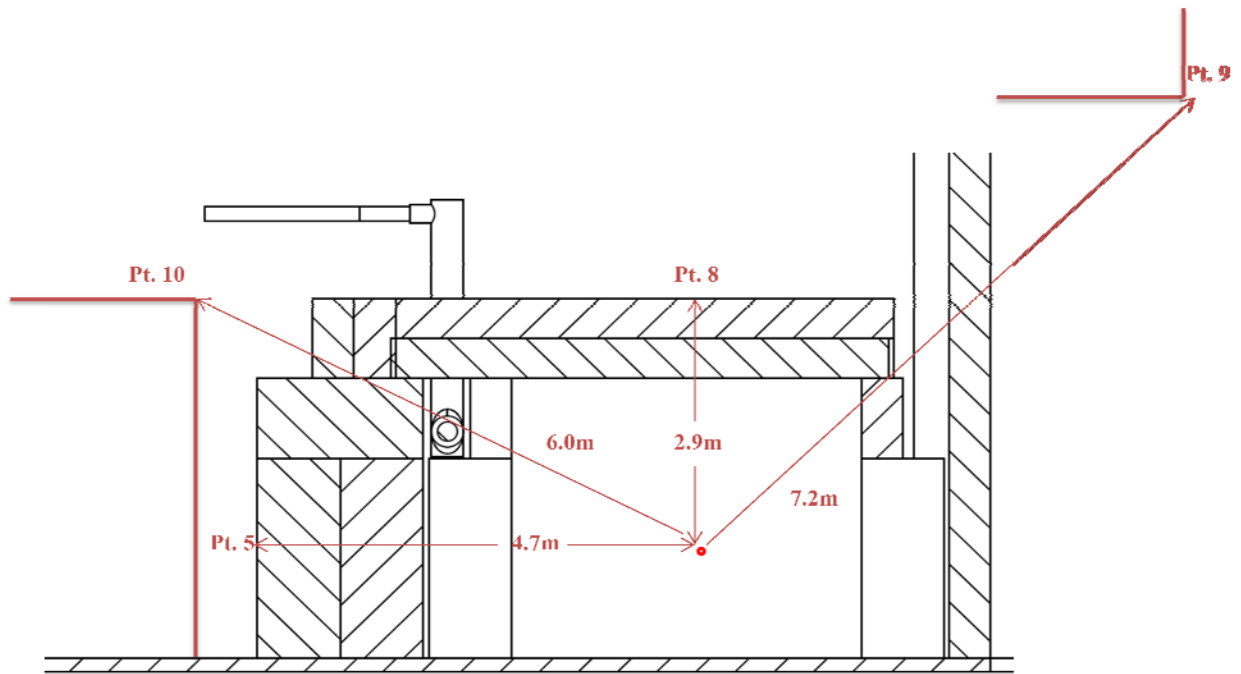


Figure 4.5: Cross section of tunnel enclosure at dose pts. 5, 8, 9, and 10.